J. Math. Kyoto Univ. (JMKYAZ)
46-3 (2006), 637–655

A lower estimate of the topological entropy from a one-dimensional reconstruction of time series

By

Maria Vivien V. Visaya

Abstract

We present a method for estimating the measure of complexity of an unknown dynamical system by studying the time series observed from it. In particular, we propose a simple method for giving a lower bound to the topological entropy of the unknown dynamical system via a one-dimensional multivalued map obtained from the time series. We illustrate this method using the Hénon map and the magnetoelastic ribbon data.

1. Introduction

Consider a sequence $\{x_n\}_{n\in\mathbb{N}}$ of successive iterates of a point $x_0 \in \mathcal{M}$ by some unknown dynamical system $f : \mathcal{M} \to \mathcal{M}$, where $\mathcal{M}$ is a bounded domain in $\mathbb{R}^d$ or a finite dimensional compact manifold. A sequence of real numbers $\{u_n\}_{n\in\mathbb{N}}$ is given as follows by an observation of $\{x_n\}$. The orbit of the form

$$n \mapsto x_n = f^n(x_0)$$

has a complete description of the evolution starting at x_0, while

$$n \mapsto u_n = \rho(f^n(x_0))$$

contains only partial information about the orbit [17]. However, $\{x_n\}$ is often difficult to observe, so understanding $\{u_n\}$ is crucial if we want to infer some interesting idea about how the *true* underlying system behaves. For instance, if we know that the observed $\{u_n\}$ has a complex behaviour, then we may say that it comes from a complex nature of $\{x_n\}$, modelled by a continuous map $\rho : \mathcal{M} \to \mathbb{R}$ which assigns to each state $x_n \in \mathcal{M}$ the corresponding observation $\rho(x_n) \in \mathbb{R}$.

The notion of topological entropy, an invariant quantitative measure of the complexity of a dynamical system f, is often used to define chaos. It measures

2000 *Mathematics Subject Classification*(*s*). 37B10, 37B40, 37M10
Received February 3, 2006

the extent to which points that are very near are mapped to points that are far away by repeated application of f. A dynamical system f may be said to be chaotic if its topological entropy, denoted by $h_{\text{top}}(f)$, is positive. For continuous maps on a compact metric space, $h_{\text{top}}(f)$ is given by the standard definition due to Bowen [3].

In this paper, we present a means of estimating a lower bound of the topological entropy of f via a time series $\{u_n\}$. In doing so, we employ the method of time-delay reconstruction and consider a set-valued map, which we shall refer to as a *multivalued map*, obtained from the time series. We then give a condition on the multivalued map that implies the positivity of $h_{\text{top}}(f)$.

There are a number of literature on reconstruction that estimate the minimum embedding dimension (e.g., [5], [13] and [14]). However, there is no standard method in choosing such. The purpose of this paper is to show that in some cases, a one-dimensional reconstruction is enough to say something about the complexity of the unknown dynamical system f. The following definitions are important to understand our results.

Definition 1.1. Let X and Y be arbitrary sets. A *multivalued map F from X to Y*, denoted by $F : X \rightrightarrows Y$, is such that $F(x)$ is assigned a set $Y_x \subset Y$ for all $x \in X$. Let

1. $\text{dom}(F) = \{x \in X \mid F(x) \neq \emptyset\}$,
2. $F(X') = \bigcup\{F(x) \mid x \in X'\}$ for $X' \subset X$.

A single-valued map $g : X'(\subset X) \to Y$ is called a *selector for F over X'* if $g(x) \in F(x)$ for all $x \in X'$.

Definition 1.2. Let X and Y be topological spaces and let $F : Y \rightrightarrows Y$ be a multivalued map. Let $f : X \to X$ and $q : X \to Y$ be continuous single-valued maps. The following diagram is said to *upper-semicommute* if $q(f(x)) \in F(q(x))$ holds for any $x \in X$:

$$\begin{array}{ccc} & \overset{f}{} & \\ X & \longrightarrow & X \\ q\downarrow & {\scriptstyle F} & \downarrow q \\ Y & \rightrightarrows & Y \end{array}$$

In the setting given above, namely given $f : \mathcal{M} \to \mathcal{M}$ and $\rho : \mathcal{M} \to \mathbb{R}$, let $I = \rho(\mathcal{M})$ be the image of ρ. We then define a multivalued map $\mathcal{F} : I \rightrightarrows I$ by

$$\mathcal{F}(x) = (\rho \circ f)(\rho^{-1}(x)) \tag{1.1}$$

such that the diagram

$$\begin{array}{ccc} & \overset{f}{} & \\ \mathcal{M} & \longrightarrow & \mathcal{M} \\ \rho\downarrow & {\scriptstyle \mathcal{F}} & \downarrow \rho \\ I & \rightrightarrows & I \end{array} \tag{1.2}$$

upper-semicommutes. Thus, for a time series $\{u_n\}$ given by $u_n = \rho(x_n) = \rho(f^n(x_0))$, it follows that the relation between $\mathcal{F}$ and $\{u_n\}$ is such that $u_{n+1} \in \mathcal{F}(u_n)$.

Definition 1.3. Let $\mathcal{F} : \mathbb{R} \rightrightarrows \mathbb{R}$ be a multivalued map and let J, K be compact intervals. Let $\partial^-(J)$ and $\partial^+(J)$ denote the left and right boundaries of J, respectively, and let $K^- = \{x \mid x < \min(K)\}$ and $K^+ = \{x \mid x > \max(K)\}$. The interval J is said to *$\mathcal{F}$-cover* K if the following conditions are satisfied:

1. $\mathcal{F}(J) \Supset K$, namely $\operatorname{int}(\mathcal{F}(J)) \supset K$;
2. $\mathcal{F}(\partial^-(J)) \subset K^-$ (resp., K^+) and $\mathcal{F}(\partial^+(J)) \subset K^+$ (resp., K^-); and
3. there exists a continuous selector for $\mathcal{F}$ over J.

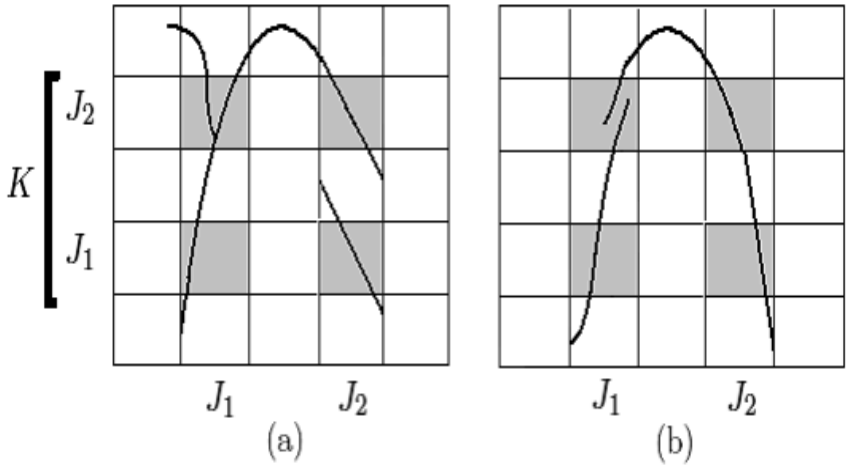

Figure 1. (a) Intervals J_1 and J_2 do not $\mathcal{F}$-cover K because condition 2 is not satisfied. (b) Interval J_1 does not $\mathcal{F}$-cover K because condition 3 is not satisfied.

Theorem 1. *Let $\mathcal{M}$ be a path-connected compact metric space. Let $f : \mathcal{M} \to \mathcal{M}$ be continuous, $\rho : \mathcal{M} \to \mathbb{R}$ continuous and onto an interval I, and $\mathcal{F} : I \rightrightarrows I$ be a multivalued map that makes diagram* (1.2) *upper semi-commutative. Assume that*

$(*)$ *there exist disjoint compact subintervals $J_1, J_2, \ldots, J_\ell$ of I and $K \supset J_1 \cup J_2 \cup \ldots \cup J_\ell$ such that for any $i = 1, 2, \ldots, \ell$, J_i $\mathcal{F}$-covers K.*

Then $h_{\mathrm{top}}(f) \geq \log \ell$.

The basic idea of Theorem 1 is that given a time series $\{u_n\}$ observed from f and a multivalued map $\mathcal{F}$ obtained from $\{u_n\}$, we can say something about

the complexity of the true underlying system f as long as there is horseshoe-like dynamics present in $\mathcal{F}$. Given $\{u_n\}$, we plot in a two-dimensional phase space points of the form $z_n = (u_n, u_{n+k})$, with some $k \geq 1$. This is how we shall view a multivalued map $\mathcal{F}^k : I \rightrightarrows I$ (see Section 4.2 for more details). For $k = 2$, we illustrate in Figure 2 the reconstruction plot of the Hénon map and magnetoelastic ribbon2 data which exhibit such horseshoe-like dynamics, as shown in Section 5.

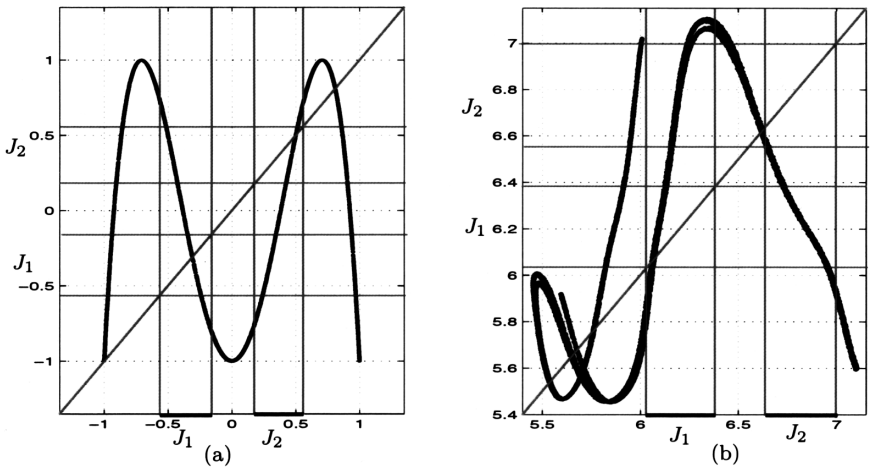

Figure 2. (a) Full shift for the second iterate of the reconstructed Hénon map with $a = 1.998$ and $b = 0.001$. (b) Subshift for the second iterate of the reconstructed magnetoelastic ribbon2 data.

This paper is organized as follows. In Section 2, we introduce the definition and some useful properties of the topological entropy. In Section 3, we give a proof of Theorem 1 together with another theorem that deals with the subshift of finite type. In Section 4, basic terminologies on time series reconstruction are discussed. The basic setting needed for the theorems applied to a time series is given as well. In Section 5, an application to the Hénon map and magnetoelastic ribbon data is presented. We give concluding remarks in Section 6.

2. Topological entropy

We give the standard definition of the topological entropy due to Bowen [3].

Definition 2.1. Let (X, d) be a compact metric space with distance d and let $g : X \to X$ be continuous. For any integer $k \geq 1$, define the distance function $d_k : X \times X \to \mathbb{R}_{\geq 0}$ by

$$d_k(x, y) = \max_{0 \leq \ell < k} d(g^\ell(x), g^\ell(y)).$$

A finite set $E \subset X$ is called (k,δ)-*separated* if $d_k(x,y) \geq \delta$ for all $x, y \in E$. Moreover, if E has the maximal cardinality among all the (k,δ)-separated sets, then E is called a *maximal* (k,δ)-*separated set*. The topological entropy of g is given by

$$h_{\mathrm{top}}(g) = \lim_{\delta \to 0} \limsup_{k \to \infty} \frac{\log s_g(k,\delta)}{k},$$

where $s_g(k,\delta)$ is the cardinality of the maximal (k,δ)-separated set for g.

We mention some useful properties of the topological entropy [11].

(1) Let X be a compact metric space and let $f : X \to X$ be continuous. Then

$$h_{\mathrm{top}}(f^m) = m h_{\mathrm{top}}(f) \text{ for every } m \in \mathbb{N}. \tag{2.3}$$

(2) Let X and Y be compact metric spaces, and let $f : X \to X$ and $g : Y \to Y$ be continuous maps. If f is semi-conjugate to g, namely there exists a continuous onto map $\varphi : X \to Y$, then

$$h_{\mathrm{top}}(f) \geq h_{\mathrm{top}}(g). \tag{2.4}$$

(3) For an integer $\ell \geq 2$, let

$$\Sigma_\ell^+ = \{s = (s_0, s_1, s_2, \ldots, s_n, \ldots) \mid s_i \in \{1, 2, \ldots, \ell\} \text{ for all } i \in \mathbb{N}\}.$$

The shift map $\sigma : \Sigma_\ell^+ \to \Sigma_\ell^+$ is such that $(\sigma(s))_n = s_{n+1}$ for $n \geq 0$. The pair (Σ_ℓ^+, σ) is called the symbol space on ℓ symbols or the full (one-sided) ℓ-shift space. The topological entropy of $\sigma : \Sigma_\ell^+ \to \Sigma_\ell^+$ is given by

$$h_{\mathrm{top}}(\sigma) = \log \ell. \tag{2.5}$$

(4) For one-sided shifts, we can also define subshifts of finite type. Given a transition matrix $A = (a_{ij})$ with $a_{ij} \in \{0, 1\}$, let

$$\Sigma_A^+ = \{s \in \Sigma_\ell^+ \mid a_{s_k, s_{k+1}} = 1 \text{ for } k = 0, 1, 2, \ldots\}.$$

Notice that Σ_A^+ is invariant under the shift map σ. Define $\sigma_A = \sigma|_{\Sigma_A^+}$. The pair (σ_A, Σ_A^+) is called the subshift of finite type for the matrix A. The topological entropy of $\sigma_A : \Sigma_A^+ \to \Sigma_A^+$ is given by

$$h_{\mathrm{top}}(\sigma_A) = \log \mathrm{sp}(A) \tag{2.6}$$

where $\mathrm{sp}(A)$ is the spectral radius of A.

3. Proof of Theorem 1

We consider the case $\ell = 2$. The proof can be readily extended to the general case and is treated in exactly the same manner. Let $\rho^{-1}(J_i) = \mathcal{N}_i$ and let $\rho^{-1}(\partial(J_i)) = \mathcal{L}_i$ for any $i = 1, 2$. Then by the continuity of ρ, the

compactness of the disjoint intervals, and the boundedness of $\mathcal{M}$, each $\mathcal{N}_i$ is compact and $\mathcal{N}_1 \cap \mathcal{N}_2 = \emptyset$. Figure 3 shows possible pre-images of J_1 and J_2 in $\mathcal{M}$. However, in general, the structure of $\mathcal{N}_i$ can be more complicated. For instance, Figure 4 illustrates a possibility of the pre-image in $\mathcal{M}$ of J_1 given in Figure 1(a). We view $\mathcal{L}_1^- = \rho^{-1}(\partial^-(J_1))$ as two disjoint subsets of $\mathcal{N}_1$ whose image under f is mapped by ρ to opposite ends of K.

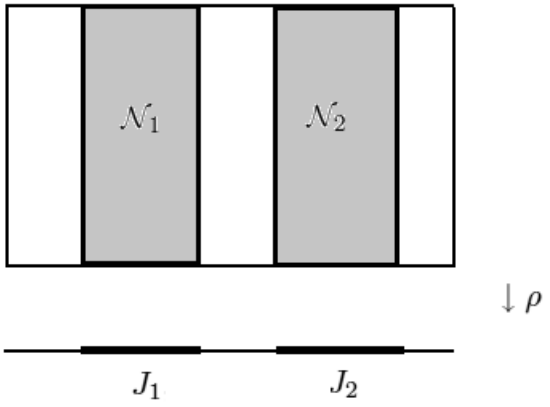

Figure 3. Pre-image in $\mathcal{M}$ for the intervals J_1 and J_2.

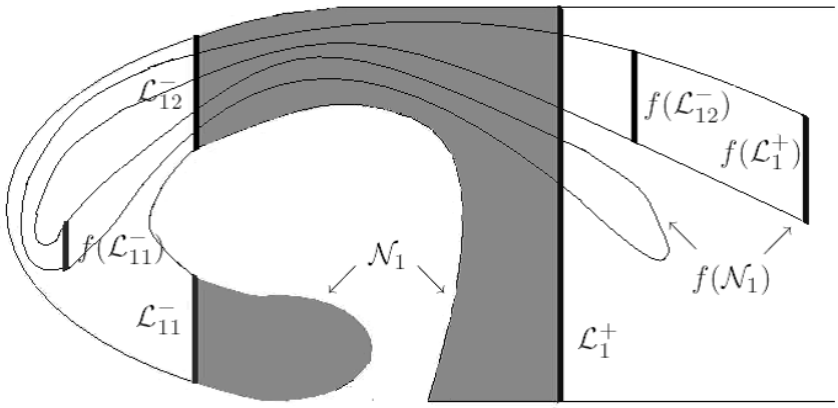

Figure 4. A possible pre-image in $\mathcal{M}$ that corresponds to $\mathcal{F}|_{J_1}$ given in Figure 1(a). The shaded region is $\mathcal{N}_1$ and the region bounded by the inner curve is $f(\mathcal{N}_1)$.

We present the following Lemma needed to prove Theorem 1.

Lemma. *There exists a continuous curve $\alpha_i : [-1, 1] \to \mathcal{N}_i$ such that*

$\rho(Im(\alpha_i)) = J_i$ *and* $\rho(\alpha_i(\pm 1)) = \partial^{\pm}(J_i)$ *for* $i = 1, 2$.

Proof. Let $\mathcal{L}_i = \mathcal{L}_i^- \cup \mathcal{L}_i^+$, where $\mathcal{L}_i^{\pm} = \rho^{-1}(\partial^{\pm}(J_i))$. Choose $x_i^{\pm} \in \mathcal{L}_i^{\pm}$. By the path-connectedness of $\mathcal{M}$, there exists a continuous path $\beta : [0, 1] \to \mathcal{M}$ connecting x_i^- and x_i^+. By the continuity of ρ, $\rho(\mathrm{Im}(\beta))$ is compact and path-connected in $\mathbb{R}$, hence an interval. If $\rho(\mathrm{Im}(\beta)) \neq J_i$, then $\rho(\mathrm{Im}(\beta)) \supsetneqq J_i$. Let

$$t^- = \max\{t \in [0, 1] \mid \beta(t) \in \mathcal{L}_i^-\},$$
$$t^+ = \min\{t \in [t^-, 1] \mid \beta(t) \in \mathcal{L}_i^+\}.$$

Clearly, $t^- < t^+$ so we obtain a path $\alpha = \beta|_{[t^-, t^+]}$ that joins $\mathcal{L}_i^-$ and $\mathcal{L}_i^+$. Reparameterizing on $[-1, 1]$, α satisfies the desired properties. □

We are now ready to prove Theorem 1.

Let $\mathcal{N} = \mathcal{N}_1 \cup \mathcal{N}_2$, $S^+ = \bigcap_{i=0}^{\infty} f^{-i}\mathcal{N}$ and $\varphi : \mathcal{N} \to \{1, 2\}$ such that $\varphi(x) = i$ if $x \in \mathcal{N}_i$. Let $\sigma : \Sigma_2^+ \to \Sigma_2^+$ be the shift map such that $(\sigma(s))_n = s_{n+1}$ for $n \geq 0$. To show that $h_{\mathrm{top}}(f) \geq \log 2$, it is sufficient to show the existence of a semi-conjugacy, namely a continuous surjective map $h : S^+ \to \Sigma_2^+$ that makes the diagram below commute.

$$\begin{array}{ccc} S^+ & \overset{f}{\longrightarrow} & S^+ \\ h \downarrow & \sigma & \downarrow h \\ \Sigma_2^+ & \to & \Sigma_2^+ \end{array}$$

Define $h : S^+ \to \Sigma_2^+$ by

$$h(x) = \big(\varphi(x), \varphi(f(x)), \varphi(f^2(x)), \ldots\big) = (s_0, s_1, s_2, \ldots) = s.$$

From the definition, h is well-defined and makes the diagram commute. For h to be surjective, we show that

$$\bigcap_{i=0}^{\infty} f^{-i}\mathcal{N}_{s_i} \neq \emptyset \tag{3.7}$$

for an arbitrary $s = (s_0, s_1, s_2, \ldots, s_n, \ldots) \in \Sigma_2^+$.

Recall that $\mathcal{N}_i \neq \emptyset$ for $i = 1, 2$. Let $\alpha_{s_0} : [-1, 1] \to \mathcal{N}_{s_0}$ be a path given in the Lemma. It is clear from the assumption $(*)$ of Theorem 1 and from the commuting diagram in (1.2) that

$$\rho(f(\mathrm{Im}(\alpha_{s_0}))) \supset (J_1 \cup J_2) \tag{3.8}$$

holds. This is illustrated for a curve α in Figure 5.

Claim. There exists a curve $\alpha_{s_0 s_1} \subset \alpha_{s_0}$ such that $\rho(f(\mathrm{Im}(\alpha_{s_0 s_1}))) = J_{s_1}$ and $\rho(f(\partial(\alpha_{s_0 s_1}))) = \partial(J_{s_1})$.

Since α_{s_0} is connected, $f(\mathrm{Im}(\alpha_{s_0}))$ is connected. Let $\rho \circ f(\alpha_{s_0}) : [-1,1] \to I$. By (3.8), $\rho(f(\mathrm{Im}(\alpha_{s_0}))) \supset J_{s_1}$. Choose $x_i^{\pm} \in \mathcal{L}_{s_1}^{\pm}$. By the same argument in the Lemma, there is a $\gamma \subset f(\mathrm{Im}(\alpha_{s_0}))$ that joins x_i^- and x_i^+. Again, as in the Lemma, we can choose $T_1 = [t_1^-, t_1^+] \subset [-1,1]$, $t_1^- < t_1^+$, such that $\rho(f(\alpha_{s_0}(T_1))) = J_{s_1}$. Defining $\alpha_{s_0 s_1} = \alpha_{s_0}|_{T_1}$, the claim follows. In particular, $\alpha_{s_0 s_1} \subset \mathcal{N}_{s_0} \cap f^{-1}\mathcal{N}_{s_1}$, and hence $\mathcal{N}_{s_0} \cap f^{-1}\mathcal{N}_{s_1} \neq \emptyset$.

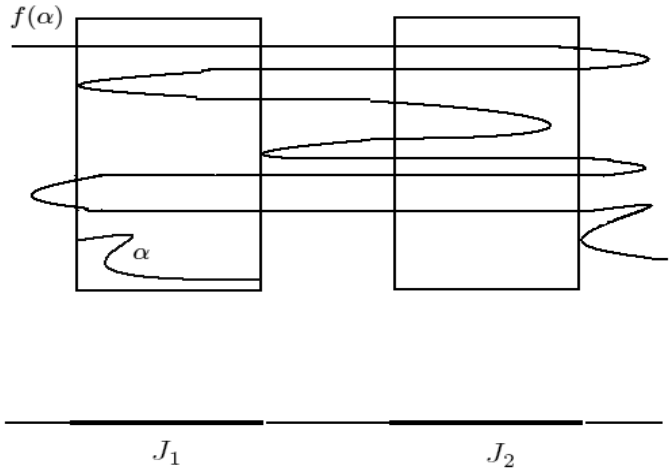

Figure 5. A curve $\alpha \subset \mathcal{N}_{s_0}$ and its image under f.

Inductively, we can construct a nested sequence of closed intervals

$$([-1,1] \supset)\ T_1 \supset T_2 \supset \ldots \supset T_k \supset \ldots,\ \ T_k = [t_k^-, t_k^+],\ t_k^- < t_k^+$$

such that $\rho(f^k(\mathrm{Im}(\alpha_{s_0}|_{T_k}))) = J_{s_k}$ and $\rho(f^k(\alpha_{s_0}(t_k^{\pm}))) = \partial(J_{s_k})$ for any k. Observe that

$$\alpha_{s_0 s_1 \ldots s_k} = \alpha_{s_0}|_{T_k} \subset \mathcal{N}_{s_0} \cap f^{-1}\mathcal{N}_{s_1} \cap \ldots \cap f^{-k}\mathcal{N}_{s_k}.$$

Since $\{T_k\}$ are compact intervals and nested, $T_\infty = \bigcap_{k=1}^{\infty} T_k$ is also a non-empty compact interval, and so

$$\alpha_{s_0}|_{T_\infty} \subset \bigcap_{i=0}^{\infty} f^{-i}\mathcal{N}_{s_i}.$$

Therefore,

$$\bigcap_{i=0}^{\infty} f^{-i}\mathcal{N}_{s_i} \neq \emptyset$$

and thus h is surjective.

Next, we show that h is continuous. Recall that the topology on Σ_2^+ is defined by the metric

$$d(s,\bar{s}) = \sum_{i=0}^{\infty} \frac{\delta_i}{2^i},$$

where

$$\delta_i = \begin{cases} 0 & \text{if } s_i = \bar{s}_i \\ 1 & \text{if } s_i \neq \bar{s}_i. \end{cases}$$

Choose $x \in S^+$ such that $h(x) = (s_0, s_1, s_2, \ldots, s_n, \ldots)$. For any $\epsilon > 0$, there exists $m \in \mathbb{N}$ such that $\frac{1}{2^m} < \epsilon$. If $s_i = \bar{s}_i$ for all $0 \leq i \leq m$, then $d(s,\bar{s}) < \frac{1}{2^m} < \epsilon$. For $x \in S^+$ and for any $k \in \mathbb{N}$, $f^k(x) \in \mathcal{N}$. From the compactness of $\mathcal{N}$, f^i is uniformly continuous on $\mathcal{N}$ for all $0 \leq i \leq m$. That is, for any $\nu > 0$, there exists $\eta = \eta_\nu > 0$ such that for any $x, y \in \mathcal{N}$,

$$d'(x,y) < \eta \quad \Rightarrow d'(f^i(x), f^i(y)) < \nu \quad \text{for all} \quad 0 \leq i \leq m,$$

where d' is the metric on $\mathcal{M}$. Let

$$v_* = \frac{1}{2} \min_{x \in \mathcal{N}_1, y \in \mathcal{N}_2} d'(x,y) > 0$$

and choose $\delta = \eta_{v_*}$. Then, for x and y with $d'(x,y) < \delta$, $h(x)$ and $h(y)$ have the same itinerary up to time m. Hence, $d(h(x), h(y)) < \frac{1}{2^m} < \epsilon$ and h is continuous for any $x \in S^+$. □

3.1. Subshift of finite type

We shall extend Theorem 1 for the subshift of finite type.

Definition 3.1. Let $\mathcal{F} : I \rightrightarrows I$ be a multivalued map on an interval I and let $\{J_1, J_2, \ldots, J_\ell\}$ be a set of compact disjoint subintervals of I. An $\ell \times \ell$ matrix $A = (a_{ij})$, $a_{ij} \in \{0,1\}$, is a *transition matrix for* $\mathcal{F}$ if for any $i = 1, 2, \ldots, \ell$, there is an interval $K_i \subset I$ such that for all $a_{ij} = 1$, the following conditions are satisfied:

1. $K_i \supset J_j$
2. J_i $\mathcal{F}$-covers K_i.

As an illustration, consider the intervals J_1, J_2, J_3 in Figure 6. Let the dark vertical lines on the left be the associated K_i for each J_i. One choice for A is

$$\mathbf{A} = \begin{bmatrix} 0 & 1 & 1 \\ 1 & 1 & 1 \\ 1 & 1 & 0 \end{bmatrix}.$$

Note that there are other choices for A. For instance, K_1 replaced with the dark vertical line on the right gives the matrix

$$\mathbf{A} = \begin{bmatrix} 0 & 1 & 1 \\ 0 & 1 & 1 \\ 1 & 1 & 0 \end{bmatrix}.$$

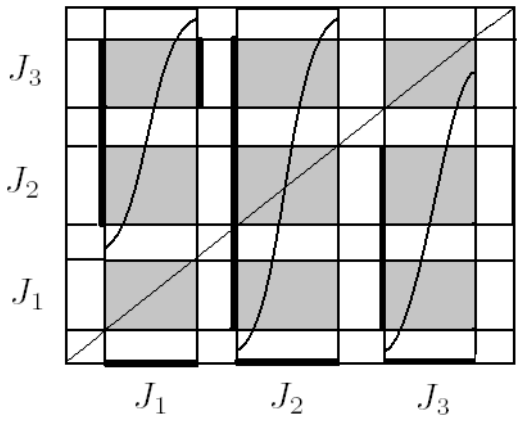

Figure 6. Associated K_i for each interval J_i, $i = 1, 2, 3$, given by the dark vertical lines.

Given a set of compact disjoint subintervals $\{J_1, J_2, \ldots, J_\ell\}$ of I and a transition matrix A for $\mathcal{F}$, we consider the one-sided subshift of finite type (σ_A, Σ_A^+). Recall that the topological entropy of the subshift is determined by the spectral radius of A, denoted by $\mathrm{sp}(A)$.

Theorem 2. *Let f, $\mathcal{M}$ and ρ be as in Theorem 1. Let $\mathcal{F} : I \rightrightarrows I$ be a multivalued map over an interval I and let $\{J_1, J_2, \ldots, J_\ell\}$ be a set of compact disjoint subintervals of I. If A is a transition matrix for $\mathcal{F}$, then $h_{top}(f) \geq \log sp(A)$.*

Given a transition matrix A for $\mathcal{F}$, let $S_A^+ = h^{-1}(\Sigma_A^+) \subset S^+$, where h is the map given in the proof of Theorem 1. By definition, S_A^+ is f-invariant. Showing that $h : S_A^+ \to \Sigma_A^+$ is a semi-conjugacy from $f|_{S_A^+}$ to $\sigma|_{\Sigma_A^+}$ is essentially the same as the proof of Theorem 1.

4. Application to time series

4.1. Time-delay reconstruction

Measuring complex systems frequently do not yield the whole set of state variables but we can infer the missing dynamics from a scalar time series by using the familiar notion of *time-delay technique*, first implemented by Packard, et al. [9]. Let $\mathcal{M} \subset \mathbb{R}^d$ be bounded, $f : \mathcal{M} \to \mathcal{M}$ and $\rho : \mathcal{M} \to \mathbb{R}$, where both f and ρ are continuous. For $m \in \mathbb{N}$, denote by Γ_ρ^m the reconstruction map of the form

$$\begin{aligned} \Gamma_\rho^m :& \mathcal{M} \to \mathbb{R}^m \\ x \mapsto& (\rho(x), \rho(f(x)), \ldots, \rho(f^{m-1}(x))). \end{aligned}$$

Essentially, only one measurable quantity is needed from the d-dimensional phase space. From the only quantity that is available, i.e., a sequence of real numbers $\{u_n\} = \{\rho(x_n)\}$, the procedure is to construct m-dimensional vectors and obtain a reconstructed set

$$\mathcal{A}_m = \overline{\{(u_i, u_{i+1}, u_{i+2}, \ldots, u_{i+(m-1)}) \mid i \in \mathbb{N}\}}.$$

For $k \geq 0$, denote by $\mathcal{A}_m^k$ the kth lag of $\mathcal{A}_m$, where

$$\mathcal{A}_m^k = \overline{\{(u_i, u_{i+k}, u_{i+2k}, \ldots, u_{i+(m-1)k}) \mid i \in \mathbb{N}\}}.$$

Figure 7 illustrates the reconstructed sets $\mathcal{A}_2$ from the Hénon map for different observation functions. With a correct choice of m, significant information about the attractor in $\mathcal{M}$ can be found by studying $\mathcal{A}_m$.

If $\mathcal{M}$ is a compact manifold with $\dim(\mathcal{M}) = D$, then for smooth $f : \mathcal{M} \to \mathcal{M}$ and $\rho : \mathcal{M} \to \mathbb{R}$, the classical embedding result due to Takens [17] states that under suitable genericity assumptions on the pair (f, ρ), if $N \geq 2D + 1$, then the map

$$\begin{aligned} \Gamma_\rho^N :& \mathcal{M} \to \mathbb{R}^N \\ & x \mapsto (\rho(x), \rho(f(x)), \ldots, \rho(f^{N-1}(x))) \end{aligned}$$

is an embedding. We shall refer to Γ_ρ^N as the embedding map and N as an embedding dimension.

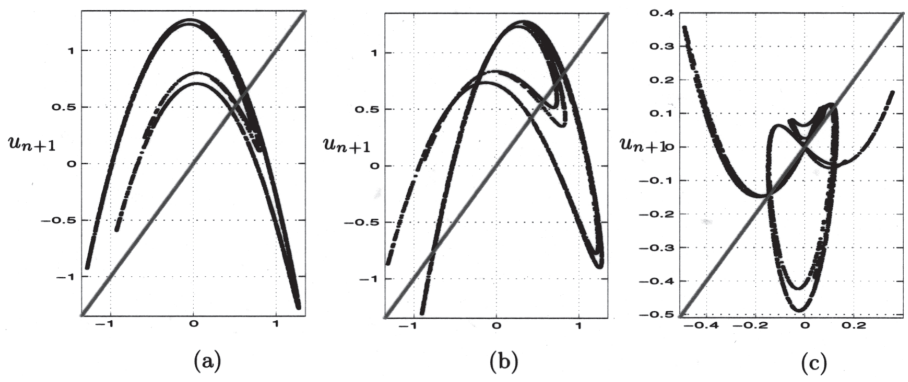

Figure 7. Reconstructed set $\mathcal{A}_2$ from the Hénon map with $a = 1.4$, $b = 0.3$, and for the observation (a) $\rho(x, y) = x$ (b) $\rho(x, y) = x + y$ and (c) $\rho(x, y) = xy$.

4.2. Basic setting

We give the basic setting in applying the theorem to a time series.

A1. There exists $f : \widetilde{\mathcal{M}} \to \mathbb{R}^d$ continuous over a bounded domain $\widetilde{\mathcal{M}} \subset \mathbb{R}^d$. Moreover, f has a closed positively invariant set $\widehat{\mathcal{M}}$ in $\widetilde{\mathcal{M}}$.

Note that we view f to model a time evolution of some phenomenon. In particular, we consider the closed positively invariant set $\widehat{\mathcal{M}}$ as an object of interest carrying some interesting phenomena. We require $\widehat{\mathcal{M}}$ to be closed in order to assure that it lies strictly inside $\widetilde{\mathcal{M}}$. Hence, f defines a dynamical system on a compact metric space $\widehat{\mathcal{M}}$.

For $x_0 \in \widehat{\mathcal{M}}$, denote the positive limit set of x_0 by

$$L^+(x_0) = \{y \in \widehat{\mathcal{M}} \mid \exists\, \{n_i\} \subset \mathbb{N}, \text{ with } n_i \in \mathbb{N} \text{ and } \lim_{i\to\infty} n_i = \infty \text{ such that } \lim_{i\to\infty} f^{n_i}(x_0) = y\}.$$

Since we are interested in a complicated dynamics in $\widehat{\mathcal{M}}$, one way to describe the dynamics of f is by looking at an orbit that, in particular, exhibits a chaotic behaviour. By definition, $L^+(x_0)$ captures the asymptotic behaviour of the phenomenon. Therefore, we often consider $L^+(x_0)$ to contain some chaotic dynamics. Moreover, since $\overline{\mathcal{O}^+(x_0)} \subset \widehat{\mathcal{M}}$, $L^+(x_0)$ is a compact invariant subset of $\widehat{\mathcal{M}}$.

A2. There exists a path-connected positively invariant compact neighborhood $\mathcal{M}$ of $\mathcal{L}^+(x_0)$ in $\widetilde{\mathcal{M}}$.

Since $L^+(x_0)$ can be viewed as some kind of an attractor, it attracts some neighborhood of it, say $\mathcal{M} \subset \widetilde{\mathcal{M}}$. In an ideal setting, we are tempted to take $\mathcal{M}$ as $L^+(x_0)$. But to be certain that $\mathcal{M}$ is path-connected, we take $\mathcal{M}$ to be a neighborhood of $L^+(x_0)$.

Notice that, in general, the assumption **A2** may not be satisfied if $L^+(x_0)$ is not connected. We show a way to give an evidence for this assumption in an example studied in Section 5. Once this is accepted, it follows that $I = \rho(\mathcal{M})$ is connected, hence I is an interval, and the multivalued map $\mathcal{F} : I \rightrightarrows I$ is defined by (1.1).

In the case where the physical system is a flow $\phi : \mathbb{R} \times \mathcal{M} \to \mathcal{M}$, we consider $f : \mathcal{M} \to \mathcal{M}$ as the time τ map given by $f(x) := \phi(\tau, x)$. For a positive orbit $\{x_n\}_{n\in\mathbb{N}}$, $x_0 \in \mathcal{M}$, each x_n is taken at a regular interval $\tau > 0$, namely $x_n = f^n(x_0) = \phi(n\tau, x_0)$.

In experiments, it is reasonable to assume that the observations are taken after transient behaviour has passed, i.e., $\mathcal{O}^+(x_0) = \{x_n\}_{n\geq 0}$ is close to the attractor $L^+(x_0)$, hence $\{x_n\} \subset \mathcal{M}$. Since the time series $\{u_n\}$ is obtained from an orbit $\{x_n\}$ in $\mathcal{M}$, if we reconstruct it in two-dimension, we expect that the reconstructed points $\overline{\{(u_n, u_{n+1})\}}_{n\in\mathbb{N}}$, which is a much smaller set in $\mathbb{R}^2$, distribute in $\Gamma^2_\rho(\mathcal{M})$.

For applications, we view this set $\mathcal{A}_2 = \overline{\{(u_n, u_{n+1})\}}$ as the graph of the multivalued map $\mathcal{F}$. The following is an argument that supports this view. Recall that

$$\text{graph}(\mathcal{F}) = \{(x, y) \mid x \in I = \rho(\mathcal{M}), y \in \mathcal{F}(x)\}.$$

Thus, by the upper-semicommutative diagram (1.2), $\mathcal{A}_2$ is contained in the graph of $\mathcal{F}$. On the other hand, since the attractor $\mathcal{A}$ we consider is the limit set $L^+(x_0)$ of the orbit $\{x_n\}$ and $\mathcal{M}$ is a small neighborhood of $\mathcal{A}$, it is reasonable in practice to assume that $\{x_n\}$ is "almost dense" in $\mathcal{M}$, namely it captures most of $\mathcal{M}$. Therefore, the reconstructed attractor $\mathcal{A}_2 = \Gamma^2_\rho(\mathcal{A})$ is approximately the same as $\mathcal{M}_2 = \Gamma^2_\rho(\mathcal{M})$, which means that any point $(x, y) \in \mathcal{M}_2$ can be approximated by a point in $\mathcal{A}_2$. Take any point $(x, y) \in \mathrm{graph}(\mathcal{F})$. Then from the definition that $\mathcal{F} = \rho \circ f \circ \rho^{-1}$, there exists $\xi \in \mathcal{M}$ such that $x = \rho(\xi)$ and $y = \rho(f(\xi))$, or equivalently, $(x, y) = \Gamma^2_\rho(\xi)$. Since $\{x_n\}$ is "almost dense" in $\mathcal{M}$, there should be an x_n which is close to ξ, and hence (x, y) is close to $\Gamma^2_\rho(x_n) = (u_n, u_{n+1}) \in \mathcal{A}_2$. This shows that $\mathrm{graph}(\mathcal{F})$ is contained in $\mathcal{M}_2 = \Gamma^2_\rho(\mathcal{M})$ which is, in practice, approximately equal to $\mathcal{A}_2$. Thus we have approximately the opposite inclusion and hence, it is justified that at least in applications, it is reasonable to consider $\mathcal{A}_2$ as the graph of the multivalued map $\mathcal{F}$.

With these assumptions, we have the following correspondence: the unknown dynamical system f corresponds to the multivalued map $\mathcal{F}$; the attractor $\mathcal{A} = L^+(x_0)$ in $\mathcal{M}$ corresponds to $\mathcal{A}_2$; and the orbit $\{x_n\}$ converging to $\mathcal{A}$ corresponds to the observation $\{u_n\}$.

5. Examples

5.1. The Hénon map

We first consider the two-dimensional Hénon map given by

$$\begin{aligned} x_{n+1} &= 1 + y_n - a x_n^2 \\ y_{n+1} &= b x_n \end{aligned} \tag{5.1.1}$$

with initial value $(x_0, y_0) = (0, 0)$. Denote by $\mathcal{H} : I \rightrightarrows I$ the multivalued map from an observation of the Hénon map. As mentioned in Section 4.2, we view the graph of $\mathcal{H}$ as the reconstruction plot of the points that are of the form $z_n = (u_n, u_{n+1})$.

Although it does not matter in principle what set of variables is used in choosing ρ to do the reconstruction, we obtain a good representation of the true attractor for the Hénon map for $\rho(x_n, y_n) = x_n$, as depicted in Figure 7(a). This is because the Hénon map in equation (5.1.1) can be written as a second order one-dimensional difference equation given by

$$x_{n+1} = b x_{n-1} + 1 - a x_n^2.$$

Thus, in such a case, the reconstructed set exhibits the exact dynamics of the real system, provided that a good observation function is chosen.

Figures 7 and 8 illustrate the graphs of $\mathcal{H}$ and $\mathcal{H}^2$ for parameters $a = 1.4$, $b = 0.3$, and for three different observation functions. Although we do not find intervals that satisfy assumption $(*)$ given in Theorem 1 for this choice of parameter values, the existence of the intervals is clear for $\mathcal{H}^2$ for parameters

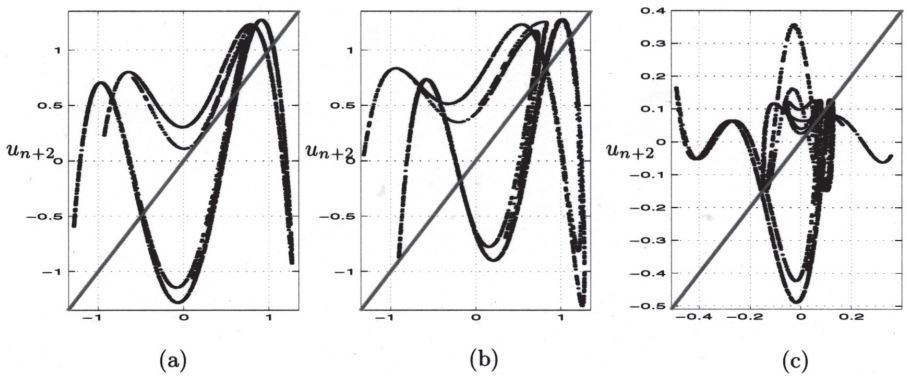

Figure 8. Reconstructed set $\mathcal{A}_2^2$ from the Hénon map with $a = 1.4$, $b = 0.3$, and for the observation (a) $\rho(x, y) = x$ (b) $\rho(x, y) = x + y$ and (c) $\rho(x, y) = xy$.

$a = 1.998$, $b = 0.001$, and observation $\rho(x_n, y_n) = x_n$, as depicted in Figure 2(a).

5.2. The magnetoelastic ribbon

The following example is an application to a time series data coming from a true experiment courtesy of J. Reiss and K. Mischaikow.

The magnetoelastic ribbon is a thin strip of magnetic material whose shape can be changed by applying a magnetic field to it. This strong coupling between strain and magnetization leads to interesting dynamics. Depending upon the parameters (i.e., the strength of the applied uniform field $\mathrm{H_{dc}}$, the strength and frequency f of the applied oscillating field $\mathrm{H_{ac}}$ in the vertical direction), the motion of the ribbon may exhibit a wide variety of different behaviours.

The dynamics of the ribbon was driven by both DC and AC magnetic fields provided by three mutually orthogonal pairs of Helmholtz coils. The position of the ribbon once per driving period is considered, and the data set consists of consecutive voltage readings from a photonic sensor. For further information concerning the experimental setup, see [10].

We consider two distinct ribbon data which we refer to as ribbon1 and ribbon2. The parameters for ribbon1 are $\mathrm{H_{dc}} = 2212.4542$ mV, $\mathrm{H_{ac}} = 3200$ mV and a driving frequency $f = .95$ Hz. The parameters for ribbon2 are $\mathrm{H_{dc}} = 2825.3968$ mV, $\mathrm{H_{ac}} = 2840$ mV and $f = .95$ Hz. Both consist of $10,000$ data points.

For the ribbon1 data, Figure 9 illustrates the reconstruction plot for the lags $k = 1$ and $k = 2$. For the third iterate $\mathcal{F}^3$ (refer to Figure 10), we can find J_1 and J_2 that satisfy assumption $(*)$ in Theorem 1. Although not seen in Figure 10(b), we assume the existence of a continuous selector for $\mathcal{F}$ over the intervals J_1 and J_2 since ideally, the reconstructed attractor is the closure of infinitely many reconstructed points in $\mathbb{R}^2$. Moreover, with the implicit

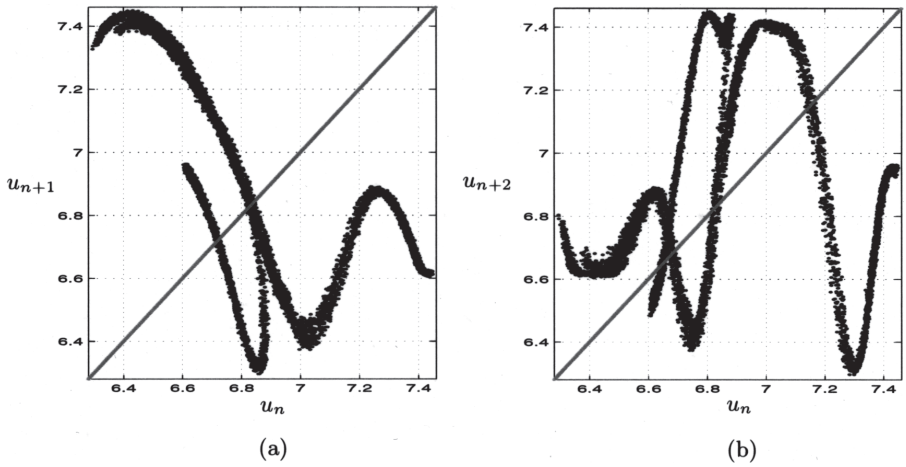

Figure 9. Reconstruction plot for the magnetoelastic ribbon1 data with lag (a) $k = 1$ (b) $k = 2$. (Data courtesy of J. Reiss.)

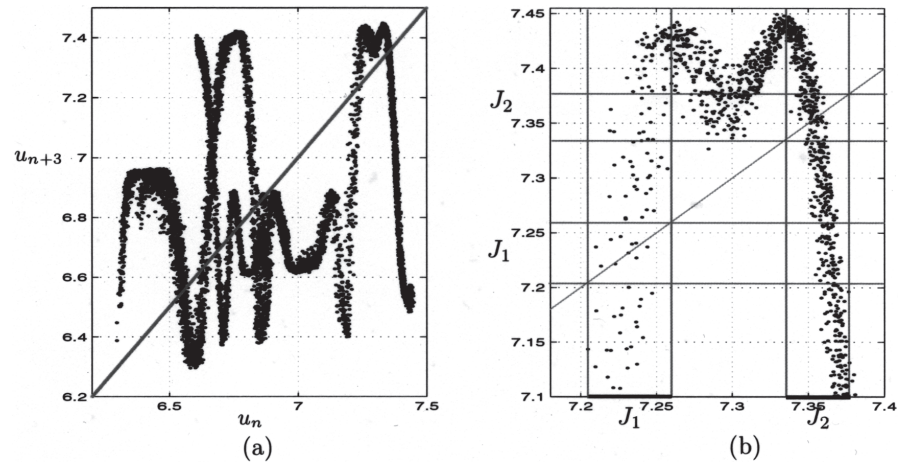

Figure 10. (a) Reconstruction plot for the magnetoelastic ribbon1 data with lag $k = 3$. (b) Intervals that satisfy $(*)$.

assumption that further increasing the number of data points n will not alter the intervals that satisfy $(*)$ for $\mathcal{F}^3$, we thus have $h_{\text{top}}(f) \geq \frac{1}{3}\log 2$.

In [8] and [16], the existence of symbolic dynamics for ribbon1 is detected from an isolating neighborhood composed of four mutually disjoint two-dimensional subsets $\mathcal{B}_i$, $i = 1, 2, 3, 4$, with the associated transition matrix given

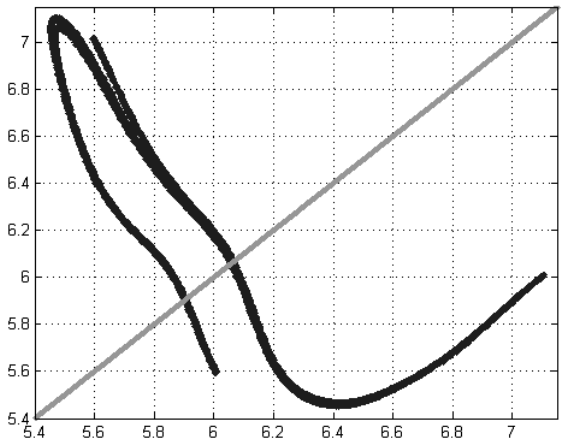

Figure 11. Reconstruction plot for the magnetoelastic ribbon2 data with lag $k = 1$. (Data courtesy of K. Mischaikow.)

by

$$\mathbf{T} = \begin{bmatrix} 0 & 0 & 0 & 1 \\ 0 & 1 & 1 & 0 \\ 1 & 0 & 0 & 0 \\ 0 & 1 & 1 & 0 \end{bmatrix}.$$

This agrees with the itinerary of $J_1 = [7.2047, 7.2677]$ for $k = 3$. In particular, $\mathcal{B}_4$ lies in the rectangle $R = \{(x, y) | 7.15 \leq x \leq 7.26, \text{ and } 6.6 \leq y \leq 6.9\}$ in Figure 17 of [16], and so a part of $\mathcal{B}_4$ whose x coordinate lies in J_1 covers itself under the third iterate, as suggested by an admissible periodic sequence $\mathcal{B}_4 \to \mathcal{B}_1 \to \mathcal{B}_3 \to \mathcal{B}_4$. This further supports our estimate for the lower bound of $h_{\text{top}}(f)$.

For the ribbon2 data, the reconstruction plot for lag $k = 1$ is illustrated in Figure 11. Although there are no intervals for which a horseshoe exists for the full shift, we did find a subshift of finite type for the second iterate, associated with the matrix

$$\begin{bmatrix} 1 & 1 \\ 1 & 0 \end{bmatrix}$$

as depicted in Figure 2(b). In this case, $h_{\text{top}}(f) \geq \frac{1}{2}\left(\frac{1+\sqrt{5}}{2}\right)$.

We now verify assumption **A2**. In particular, we want to obtain information about the path-connectedness of $\mathcal{M}$ only from the observed time series $\{u_n\}$. One approach to this problem is to compute a topological invariant, called the Betti number. Note that to a topological space X, one can assign

homology groups $H_i(X), i = 0, 1, 2, \ldots$. Betti numbers, which we denote as β_i, are the rank of $H_i(X)$. For $k = 0$, β_0 counts the number of connected components of X. In particular,

$$X \text{ is connected } \Leftrightarrow \beta_0 = 1.$$

The zeroth Betti number is therefore the type of information we seek, particularly in verifying assumption **A2**. Note that in this context, since $\mathcal{M}$ is a neighborhood, the path-connectedness and connectedness of $\mathcal{M}$ are the same.

For practical verification, computation of β_0 is carried out using the CHomP software [18]. The reconstructed set in $\mathbb{R}^m$ is approximated by a cubical set, that is, a union of finitely many m-cubes. The procedure is to grid $\mathbb{R}^m$ into m-dimensional boxes and consider the set of all boxes that contain the data points. We refer to [6] for the complete description of the algorithm. For the ribbon1 and ribbon2 data, a 50×50 cubical grid composed of grid squares of size 0.023070 and 0.033136 respectively, give $\beta_0 = 1$ for $m = 2$ and $m = 3$. In principle, if the data size is large enough, one can continue this procedure for larger m and finer grid size, and obtain a more convincing conclusion on the connectedness of $\mathcal{A} = L^+(x_0)$. Of course, in practice, this procedure cannot give a mathematical proof due to the limitation that one can only deal with finite (relatively low) m and finite (though large) data points.

Note that if the reconstruction is an embedding, then the conclusion about the connectivity of $\mathcal{A}$ is clear since the properties of $\mathcal{A}$ is mirrored in $\mathcal{A}_N$, where N is an embedding dimension. The problem is that the dimension D of the true dynamical system f is usually unknown. Although there are statistical methods for identifying D, a reasonable estimate of the true dimension is difficult to compute from experimental data. Despite the practical assumption that the number of data points is large enough, in theory, D is a limit that is reached only with infinite data. Furthermore, in the case where D is known, it may happen that $N = 2D+1$ is too large and thus presents the difficulty in visualizing $\mathcal{A}_N$.

6. Conclusions

We have presented a method for showing the positivity of the topological entropy of the unknown dynamical system from a one-dimensional reconstruction of time series. By constructing a one-dimensional multivalued map $\mathcal{F}$ obtained from a time series $\{u_n\}$, we can give a lower estimate for the topological entropy of the true dynamical system f, provided there is horseshoe-like dynamics in $\mathcal{F}$.

The advantage of the method presented lies in the fact that we *do not need* the reconstruction map to be an embedding. We detect symbolic dynamics through the disjoint intervals satisfying the assumptions in either of the theorems and show that the true system f is at least as complicated as that of the one-sided full shift or subshift of finite type.

It is worth noting the result of Mischaikow, et al. ([7], [8]) that is likewise independent of the embedding dimension. In their work, they consider a multivalued map $F : \mathcal{G} \rightrightarrows \mathcal{G}$, $\mathcal{G} \subset \mathbb{R}^2$, that takes squares to a set of squares.

We have further simplified studying the dynamics in the one-dimensional case by considering a one-dimensional multivalued map $\mathcal{F} : I \rightrightarrows I$ defined by (1.1) such that for a given time series $\{u_n\}$, $u_{n+1} \in \mathcal{F}(u_n)$.

Note that throughout the paper, we assume that a time series data set does not contain any error. Experimental time series data, however, consists of values u_n related to the original states by

$$u_n = \rho(x_n) + \zeta_n,$$

where ζ_n denotes some inaccuracy in measuring the observations. In [7] and [8], the observation function is modelled as a multivalued map that takes into account error present in the time series. A multivalued measurement function $\theta : \mathcal{M} \rightrightarrows \mathbb{R}$ is defined such that each point $x \in \mathcal{M}$ is assigned an interval $\theta(x) = I_x \subset \mathbb{R}$, with the assumption that ρ is a continuous selector for θ.

Similarly, our method is insensitive to any small error or any small perturbation of f, say f_λ. This is due to the assumption that $\mathcal{F}(\partial(J_i))$ will always lie strictly outside K. This may be argued as well by the robustness of the horseshoe which assures that the graph of $\mathcal{F}_\lambda$ will lie close to the graph of $\mathcal{F}$ near the disjoint intervals satisfying $(*)$.

Clearly, the drawback in our method is that the application is restricted to time series data that come from an almost one-dimensional chaotic system. Furthermore, we lose information about the geometric information of the true attractor $\mathcal{A} \subset \mathcal{M}$. In particular, the topology of $\mathcal{A}$ may not be mirrored in a one-dimensional reconstruction.

Acknowledgements. This work was supported by the Scientific Research Grant-in-Aid from the Ministry of Education, Science, Sports and Culture of Japan. The author wishes to express her deep gratitude to Prof. Hiroshi Kokubu for his guidance and support, and for the many fruitful discussions which have been most helpful for the completion of this paper. She would also like to thank the referee for clarifying the structure and presentation of the paper.

Department of Mathematics
Faculty of Science, Kyoto University
Kyoto, 606-8502
e-mail: v3isaya@math.kyoto-u.ac.jp

References

[1] L. Alsedà, J. Llibre and M. Misiurewicz, *Combinatorial Dynamics and Entropy in Dimension One*, Adv. Ser. Nonlinear Dynam. **5**, 2nd ed., World Scientific, Singapore, 2000.

[2] A. Baker, *Lower bounds on entropy via the Conley index with applications to time series*, Topology Appl. **120** (2000) 333–354.

[3] R. Bowen, *Entropy for group endomorphisms and homogeneous spaces*, Trans. AMS **153** (1971) 509–510.

[4] H. W. Broer, F. Dumortier, S. J. van Strien and F. Takens, *Structures in Dynamics: Finite Dimensional Deterministic Studies*, North-Holland, 1991.

[5] K. Fueda and T. Yanagawa, *Estimating the embedding dimension and delay time from chaotic time series with dynamic noise*, J. Japan Statist. Soc. **31** (2001) 27–38.

[6] T. Kaczynski, K. Mischaikow and M. Mrozek, *Computational Homology*, Springer-Verlag New York, 2004.

[7] K. Mischaikow, M. Mrozek, A. Szymczak and J. Reiss, *From time series to symbolic dynamics: an algebraic topological approach*, preprint, 1997.

[8] ———, *Construction of symbolic dynamics from experimental time series*, Phys. Rev. Lett. **82** (1999) 1114–1147.

[9] N. Packard, J. Crutchfield, J. Farmer and R. Shaw, *Geometry from a time series*, Phys. Rev. Lett. **45** (1980) 712–716.

[10] J. Reiss, *The analysis of chaotic time series*, Ph. D. Thesis, Georgia Inst. Tech., Atlanta, 2001.

[11] C. Robinson, *Dynamical Systems: Stability, Symbolic Dynamics, and Chaos*, C.R.C. Press, 1994.

[12] D. Ruelle, *Chaotic Evolution and Strange Attractors*, Cambridge University Press, 1989.

[13] T. Sauer and J. Yorke, *How many delay coordinates do you need?*, Int. J. Bifur. Chaos **3** (1993) 737–744.

[14] M. Small and C. Tse, *Optimal selection of embedding parameters for time series modelling*, preprint, 2003.

[15] J. S. Sprott, *Chaos and Time Series Analysis*, Oxford University Press, 2003.

[16] A. Szymczak, *Index pairs: from dynamics to combinatorics and back*, Ph. D. Thesis, Georgia Inst. Tech., Atlanta, 1999.

[17] F. Takens, *Detecting strange attractors in turbulence*, Dynamical Systems and Turbulence, Warwick 1980, D. Rand and L. S. Young, eds., Lecture Notes in Math. **898**, Springer-Verlag, Berlin, 1981.

[18] http://www.math.gatech.edu/~chomp/software/.